Available online at www.sciencedirect.com

ScienceDirect

journal homepage: www.elsevier.com/locate/he

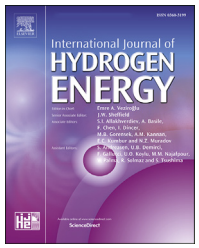

Evaluating the hydrogen storage potential of shut down oil and gas fields along the Norwegian continental shelf

Benjamin Emmel[*], *Bård Bjørkvik*, *Tore Lyngås Frøyen*, *Pierre Cerasi*, *Anna Stroisz*

SINTEF Industry, Applied Geoscience, Trondheim, Norway

HIGHLIGHTS

- First evaluation of hydrogen storage potential of shut down fields on the Norwegian continental shelf.
- Estimate of contamination risks due to residual hydrocarbons and geochemical reactions.
- Cumulative maximum theoretical hydrogen storage capacity for 23 shut down oil and gas fields of up to 642 TWh.

ARTICLE INFO

Article history:
Received 19 August 2022
Received in revised form
1 March 2023
Accepted 11 March 2023
Available online 5 April 2023

Keywords:
Hydrogen storage
Norwegian continental shelf
Oil and gas fields

ABSTRACT

The underground hydrogen storage (UHS) capacities of shut down oil and gas (O&G) fields along the Norwegian continental shelf (NCS) are evaluated based on the publicly available geological and hydrocarbon production data. Thermodynamic equilibrium and geochemical models are used to describe contamination of hydrogen, loss of hydrogen and changes in the mineralogy. The contamination spectrum of black oil fields and retrograde gas fields are remarkably similar. Geochemical models suggest limited reactive mineral phases and meter-scale hydrogen diffusion into the caprock. However, geochemical reactions between residual oil, reservoir brine, host rock and hydrogen are not yet studied in detail. For 23 shut down O&G fields, a theoretical maximum UHS capacity of ca. 642 TWh is estimated. We conclude with Frigg, Nordost Frigg, and Odin as the best-suited shut down fields for UHS, having a maximum UHS capacity of ca. 414 TWh. The estimates require verification by site-specific dynamic reservoir models.

Introduction

One of the most critical challenges in a forthcoming energy society with low carbon emissions is the storage of energy generated from renewable sources [1,2]. The generation of energy using renewable sources like wind, solar, and hydropower is intermittent, and it is essential to account for the variation in energy supply and demand between seasons [3]. To assure a stable, secure, and safe European energy supply, temporary storage of excess energy is one of the key strategies [4] to balance energy production and demand fluctuations [5].

* *Corresponding author.*
E-mail address: benjaminudo.emmel@sintef.no (B. Emmel).

https://doi.org/10.1016/j.ijhydene.2023.03.138

Energy storage must be targeted at all scales, from battery type (kWh), tanks and pipelines (MWh) to high-capacity underground reservoirs (TWh) in order to build strategic energy reserves [6]. One option is converting surplus renewable energy into hydrogen through water electrolysis [7], and then storing the produced hydrogen until the energy is needed [8]. Hydrogen can be stored on the surface, on the seabed in tanks or underground in depleted O&G fields, porous aquifers, or manufactured salt caverns [9,10] similarly to CO_2 and natural gas storage. Compared to surface storage, UHS in shut down O&G fields has several advantages: (i) huge quantities of hydrogen can be stored; (ii) the underground conditions are well characterised; (iii) field exploration and decommissioning costs can be reduced; (iv) available infrastructure might be reused; (v) safety risks related to caprock leakage and human manipulations are low; (vi) low specific investment costs per MWh of storage [11,12]. The risks of UHS are comparable to CO_2 and natural gas storage, risks which have been well described during the last decades [13]. The release of stored fluids into the biosphere and/or atmosphere can occur due to catastrophic events such as seismic or volcanic activity, seepage through fault zones or inadequate caprocks, or leakage along human-made routes such as oil and gas wells [14,15]. The primary distinction between hydrogen and CO_2 storage is in their storage duration. Hydrogen is meant to be stored temporarily (weeks/months) upon cyclic injection/retrieval, whereas CO_2 needs to be stored permanently over geological time scales [16,17]. Compared to the long-term storage of CO_2, the periodic subsurface operations for hydrogen will affect the mechanical, chemical and hydraulic properties of the storage reservoir rocks and the sealing caprocks and well barrier cement [18]. Field data can provide important information about potential hydrogen sources and loss mechanisms [19]. Ideally, a UHS reservoir is well characterised, has good reservoir and caprock units and pressure/temperature changes have been monitored over extended periods as is the case for O&G fields.

A total of 112 fields have been developed along the Norwegian continental shelf since 1971, when O&G production started in Norway. At the end of 2019, 87 fields were in production and 25 fields were shut down [20]. This paper evaluates 23 fields, excluding Murchison and Troll B, regarding their UHS potential (Fig. 1). To evaluate each field, we convert O&G production data into theoretical maximum UHS capacities. Our approach for estimating the H_2 storage capacity of shut down O&G fields follows the strategy employed by the Joule II project for CO_2 storage [21]. At first, we collect all essential geological data, including the reservoir lithologies, depths, temperatures and pressures, caprock lithologies and thicknesses. Then, we analyse and review the impact of various contaminations with (i) residual hydrocarbons that remain in a "depleted field", (ii) formation brine that remains, migrates or is injected into the reservoir, (iii) host rock that interacts with hydrogen and (iv) microbes.

Up to 80–95% of the hydrocarbons may remain in the pore space of depleted oil reservoirs when oil is extracted solely using its in-situ pressure. This can be reduced to 50% if additional water is injected into the reservoir unit [22]. In a produced natural gas field, the amount of residual gas is usually lower [23] and depends mainly on the influx of aquifer water, filling pore spaces and trapping gas. Residual hydrocarbons may react with the injected hydrogen, and parts of the residual hydrocarbon may contaminate the produced hydrogen. The impurities can become a large issue depending on the further use of hydrogen. For example, if hydrogen is intended for use in fuel cells, impurities can negatively impact fuel cell performance [24,25]. Moreover, if hydrogen purification is required after production, it can become a major cost factor [26]. So far, detailed discussion about contamination risks has been restricted to depleted dry gas reservoirs [5,27]. Considering that depleted retrograde gas (gas condensate) and oil reservoirs contribute significantly to the potential offshore UHS capacity at the NCS, we focus on the contamination issue of such storage sites. To evaluate the influence of residual hydrocarbon phases on the chemical compositions of the produced gas phases, we used thermodynamic equilibrium models and analysed the streamed hydrogen composition/purity. The inorganic geochemical reactions and hydrogen diffusion out of the UHS units are analysed using a simplified generic geochemical model. We conclude with maximum theoretical hydrogen storage capacities for the shutdown O&G fields at the NCS. Fig. 2 summarizes the workflow applied in this study.

Methods and data generation

Geochemical and equilibrium modelling

The chemical fluid composition after injecting hydrogen is modelled using the PVTSIM software (calsep.com) and is analysed for two simplified fluid compositions representative of most shut down fields. During UHS, the gas must be injected as cushion gas (the amount of gas that is permanently stored) and working gas (the gas volume that can be injected, stored, and withdrawn). In thermodynamic equilibrium models, we assume that hydrogen is utilized as both the cushion and working gas, except for two models which use CO_2 as the cushion gas. These models are applied to retrograde gas and black oil reservoirs that have been depleted to a pressure of 50 bar and a temperature of 100 °C. We assume that the front of the injected cushion gas displaces the reservoir hydrocarbon gas and water (in the case of waterflooded oil reservoir) from the region around the injection well. The lagging cushion gas equilibrates with the residual (immobile) hydrocarbon liquid phase. After the injection of cushion gas, the working gas is injected and retrieved in a cyclic manner. Here we assume (i) no mixing between the cushion and working gas and (ii) no mixing between the newly injected working gas in each cycle (perfect batch process). The composition of the working gas is estimated throughout the first three cycles using the commercial equation-of-state fluid simulator PVTSIM Nova 5 [28] employing the Soave-Redlich-Kwong Peneloux equation of state. The estimates are based on typical North Sea hydrocarbon fluid compositions. The retrograde gas has a gas-condensate ratio of approximately 1500 Sm^3/Sm^3 and contains approximately 76 mol % methane. The black oil has a gas-oil ratio approximately 90 Sm^3/Sm^3 and contains approximately 44 mol % methane.

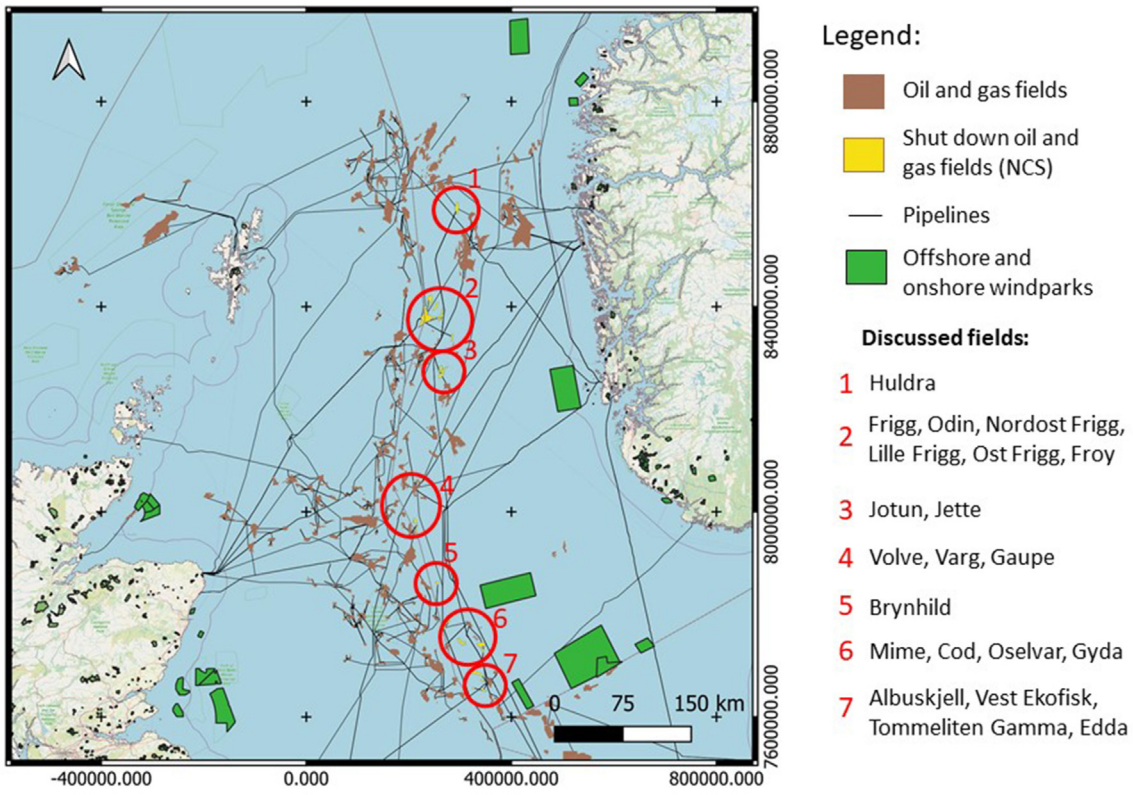

Fig. 1 – Location of O&G fields, pipelines and planned and installed wind parks in the UK and Norwegian North Sea. The red circles show the areas with shut down O&G fields; names of discussed fields are given with numbers. Yttergryta field in the Norwegian Sea is not shown on this map.

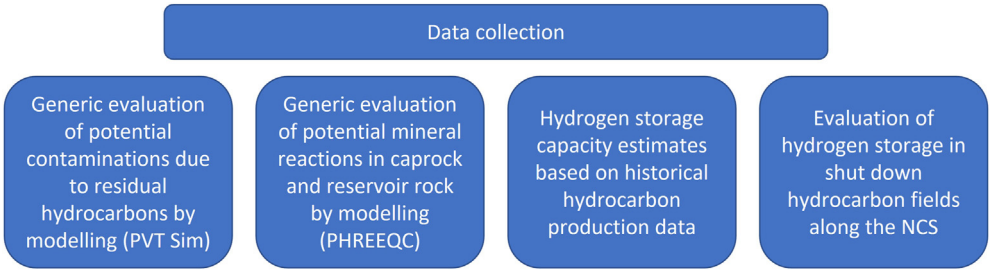

Fig. 2 – Workflow description of the study.

Inorganic hydrogen reactions (+ microbial activities) are simulated using the PHREEQC software with the phreeqc.dat thermodynamic data file [29] for a generic case. We use modal compositions of representative caprock (shale from Draupne Fm [30]) and reservoir rock units (sandstone from Froan Basin [31]). To calculate the reactive amounts of each mineral phase, the rock porosity is filled with fluids (reservoir brine, residual gas, stored gas), and the mineral-specific density is considered. We assume that only the minerals in contact with the pore space participate as reactive phases. We apply the modelling strategy described by Hemme and Van Berk [18]. The model is restricted to the reservoir/caprock boundary with a 20 m thick sandstone reservoir sealed by a 10 m thick shale caprock (with shale porosities of 9.5%, 5% and 1%). To model the reservoir and caprock fluid compositions, we assume seawater in contact with reservoir/caprock to be in a chemical equilibrium [32]. The models are performed at a reservoir pressure of ca. 200 bar and a temperature of 60 °C.

Capacity estimates

We categorized the O&G fields into gas (dry and wet gas fields), gas-prone (retrograde gas fields), oil, and black oil fields (Table 2) based on the production gas-to-oil ratio (PGOR).

$$(1)\ \mathrm{PGOR} = V_{\mathrm{Uoil(st)}}/V_{\mathrm{gas(st)}}$$

A field that produced only gas is classified as a dry gas field. The further subdivision depends on the produced amounts of O&G, with solution: PGOR >9000 = gas; 9000 > PGOR >590 = gas prone; 590 > PGOR >360 = oil; PGOR <360 = black oil (similar to [33]).

Table 1 – Assumptions for the PVTSIM models. All models are calculated at a constant pressure of 50 bar and temperature of 100 °C for one cushion gas and three working gas injection cycles.

Model ID	Initial fluid	Mixture (% H2)	Cushion gas
R95H2	Retrograde gas	95	Hydrogen
R80H2	Retrograde gas	80	Hydrogen
R50H2	Retrograde gas	50	Hydrogen
BO95H2	Black oil	95	Hydrogen
BO80H2	Black oil	80	Hydrogen
BO50H2	Black oil	50	Hydrogen
R95CO2	Retrograde gas	95	CO2
BO95CO2	Black oil	95	CO2

Maximum hydrogen storage capacity estimates

To calculate the maximum hydrogen storage capacities, we use the sum production of gross oil ($V_{oil(st)}$ in mill Sm3), gas ($V_{gas(st)}$ in bill Sm3) and condensates (from [34]). These volumes at standard conditions are back-calculated to reservoir conditions (underground volume of oil (V_{Uoil}) and gas (V_{Ugas}) using the simplified oil formation volume factor (FVF) or the gas expansion factors (GEF). Both factors are given for most shut down Norwegian O&G fields [21,35].

(2) $V_{Uoil} = V_{oil(st)}$ x FVF/1000

(3) $V_{Ugas} = V_{gas(st)}$/GEF

If FVF is not available, we use the mean value of 1.52 calculated from 20 FVFs from Norwegian oil fields [21]. For cases with unavailable GEF, we calculate the GEF using the given reservoir pressures (P) and linear relationship based on British and Norwegian well data [21].

(4) GEF = 4.8 x P + 93.1

To calculate the gravimetric hydrogen storage capacity in the underground Q_{UH2} (in a million tonnes, Mt), the density of pure hydrogen (ρUH_2 in kg/m^3) at reservoir conditions is calculated using data provided in the NIST WebBook [36].

(5) $Q_{UH2} = (V_{Ugas} + V_{Uoil})$ x ρUH_2

The calculated mass of hydrogen is converted to potential energy (in TWh) using the heating value for hydrogen (HHV) of 39.4 kWh/kg [37].

(6) $E_{UH2} = Q_{UH2}$ x 39.4

Results and interpretation

Thermodynamic equilibrium modelling of hydrogen loss and upstream impurities

The equilibrium between hydrogen and hydrocarbon is calculated for eight different models (Table 1). Three cases are modelled (i) low hydrocarbon residues (95 mol % hydrogen), (ii) intermediate hydrocarbon residues (80 mol % hydrogen), and (iii) high hydrocarbon residues level (50 mol % hydrogen) for gas condensate and black oil. Hydrogen concentrations >80 mol % are relevant for retrograde gas reservoirs, whereas concentrations <80 mol % are relevant for oil reservoirs. The two models use CO_2 instead of hydrogen as cushion gas.

The results for retrograde gas and black oil, with hydrogen as cushion gas, indicate a significant difference between the

Table 2 – Shut down fields summarizing production data, fluid characterisation and storage capacity estimates. Abbreviations: PGOR: production gas to oil ratio, Hy_Dens: hydrogen density at reservoir conditions; UHS: underground hydrogen storage capacity.

Field Name	Oil (mill sdm3)	Gas (bill sdm3)	GOR	Reservoir type	Hy_Dens (kg/m3)	UHS (Mt)	UHS (TWh)
ALBUSKJELL	9.56	17.13	1792.24	Retrograde gas	23.84	0.35	13.68
BRYNHILD	0.53	–	51.78	Black oil	28.44	0.02	0.89
COD	4.08	–	1827.76	Retrograde gas	26.05	0.16	6.37
EDDA	5.17	2.11	409.01	Volatile oil	21.17	0.17	6.57
FRIGG	–	115.87	1013277.45	Wet gas	12.93	7.76	305.83
FROY	5.88	–	294.58	Black oil	11.10	0.10	3.91
GAUPE	–	0.56	2365.24	Retrograde gas	18.65	0.04	1.52
GLITNE	8.88	–	53.61	Black oil	12.769	0.17	6.79
GYDA	41.00	–	225.67	Black oil	23.45	1.52	60.00
HULDRA	–	18.00	4430.99	Retrograde gas	4.96	0.66	25.83
JETTE	0.43	–	97.26	Black oil	10.900	0.01	0.28
JOTUN	23.14	–	55.81	Black oil	12.14	0.43	16.82
LILLE-FRIGG	–	2.26	1636.02	Retrograde gas	10.36	0.12	4.70
MIME	0.39	–	206.85	Black oil	25.08	0.01	0.59
NORDOST FRIGG	–	11.61	296894.79	Wet gas	13.07	0.77	30.35
ODIN	–	27.74	223134.40	Wet gas	13.19	1.81	71.38
OSELVAR	0.77	–	544.82	Volatile oil	24.73	0.03	1.15
OST FRIGG	–	9.42	23523.27	Wet gas	12.80	0.62	24.60
TOMMELITEN GAMMA	5.29	10.48	1982.75	Retrograde gas	22.12	0.18	7.02
VARG	16.33	–	298.47	Black oil	17.03	0.42	16.66
VEST EKOFISK	15.46	–	1811.32	Retrograde gas	22.11	0.54	21.34
VOLVE	10.07	–	143.95	Black oil	16.12	0.25	9.72
YTTERGRYTA	–	2.57	8768.25	Retrograde gas/Wet gas?	11.18	0.15	5.99

contamination levels in the cushion gas injection step and the following three working gas injection cycles (Fig. 3). In general, the hydrogen content increases and contaminants decrease during the first three injection cycles. The composition of the initial fluid (supplementary data) affects the contamination of the stored hydrogen. There is a significant difference in composition between the retrograde gas, containing more light and intermediate-weight components (C1 to C4) and the black oil, containing more heavy-end hydrocarbon components (C6 to C42-80).

At reservoir conditions, mass transfer between hydrogen and hydrocarbon phases will occur, i.e. (i) hydrogen will be dissolved/condensed into the hydrocarbon phase, and ii) hydrocarbon will be extracted/evaporated into the hydrogen phase. The equilibrated compositions of the hydrogen-rich phase (working/cushion gas) and hydrocarbon-rich phase (initial fluid occupying the pore space) depend on the initial hydrocarbon composition, reservoir pressure and temperature. In general, hydrogen will predominately extract lighter hydrocarbon components [38,39]. Consequently, more hydrocarbon components will be extracted into hydrogen for the retrograde gas compared with black oil, leading to a higher contamination level for the retrograde gas than for the black oil scenario (Fig. 3). In agreement with [38,39], the hydrogen cushion gas predominately extracts the more volatile (lighter) components of the residual hydrocarbon liquid phase (Fig. 4).

Fig. 5 shows the liquid phase composition of representative retrograde gas and black oil before (Fig. 5a) and after equilibration (Fig. 5b) with hydrogen in the cushion gas injection (Models R95H2 and BO95H2). The equilibrium hydrocarbon liquid contains approximately 4 mol % hydrogen. The hydrogen cushion gas extracts and removes a large part of the more volatile components of the residual hydrocarbon liquid phase (Fig. 4). It is noted that the contamination level is higher (lower amounts of hydrogen) for the retrograde gas than for the black oil scenario (Fig. 3).

Fig. 6 compares the contamination profiles of the first three working gas cycles using CO_2 and hydrogen as cushion gas (Models R95H2, R95CO2, BO95H2 and BO95CO2). The level of hydrocarbon contamination is less if the cushion gas is CO_2. The reduced hydrogen contamination implies that CO_2 as a cushion gas could be a cost-effective alternative method. CO_2 can extract more light and intermediate-weight components from the residual hydrocarbon liquid phase, accompanied by higher solubility of CO_2 in the hydrocarbon liquid residues. The black oil and retrograde gas scenarios using hydrogen as cushion gas give approximately 4 mol % hydrogen in the hydrocarbon liquid phase (Fig. 5). In comparison, CO_2 as cushion gas gives 6–7 times higher CO_2 concentration in the hydrocarbon liquid.

Inorganic geochemical reactions in the reservoir and caprock

The modelling results indicate a minimal hydrogen consumption related to mineral reactions in the reservoir and caprock units within the first 30 yrs (Fig. 7 a, f). Models show an increase of caprock brine pH values from ca. 7.1 to 8.7, but in the reservoir rock pH remains at its initial value of 8.7. The pH increase might trigger geochemical reactions in the caprock units.

The models indicate the dissolution of quartz, calcite, kaolinite, and k-feldspar within the first 5–10 yrs depending on the rock porosities (Fig. 7 e vs j). Illite and albite are the precipitating phases in the first 5 yrs (Fig. 7 d, i). In the 9.5% porosity model, kaolinite is dissolved in the first 5 yrs, but after 10 yrs starts to precipitate. Also, in the caprock unit quartz, calcite and kaolinite are mainly dissolved within the first 10 yrs (Fig. 7 c, h). The precipitating phase in the caprock unit is K-feldspar (Fig. 7 b, g). The amounts are negligible with e.g., the highest values for the solving phases reaching up to 0.05 mol/kgw per year of quartz which equals 1.5 g/kgw per year. Hydrogen diffusion mainly influences the first 5 m of the modelled caprock lithology (porosity of 5%) in the first 100 yrs. In longer timescales, hydrogen might diffuse through a 10 m caprock unit (Fig. 8, 1000 yrs). All presented results are case-specific and cannot be generalised.

Hydrogen storage capacities

Twenty-two fields are in the Norwegian North Sea and the Yttergryta field is in the Norwegian Sea. The reservoir rocks are mainly sandstones (19 fields); only in Vest Ekofisk, Albuskjell, Tommeliten Gamma, and Edda fields the reservoir units are chalks (supplementary data Table 3). The maximum ca-

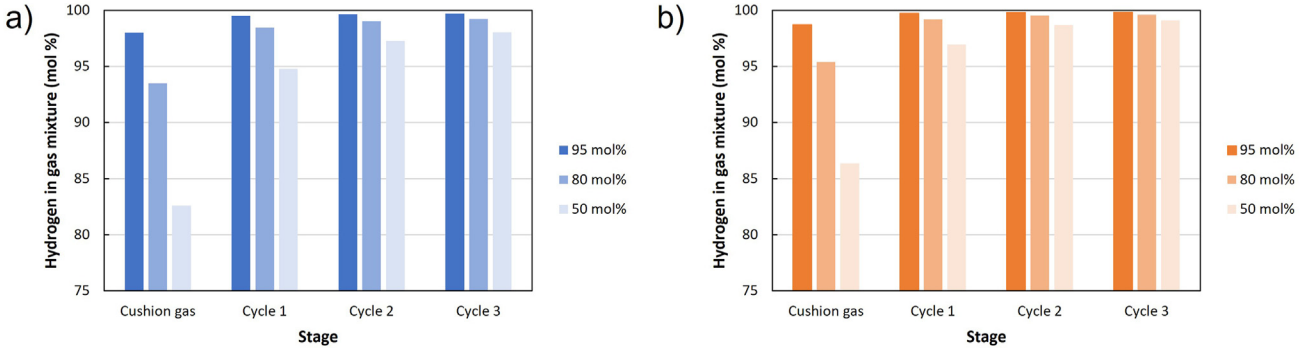

Fig. 3 – Mol percentage hydrogen in equilibrated cushion gas and three working gas cycles for retrograde gas (a) and black oil (b) scenarios with hydrogen as cushion gas and initial mol % of hydrogen in the gas mixture.

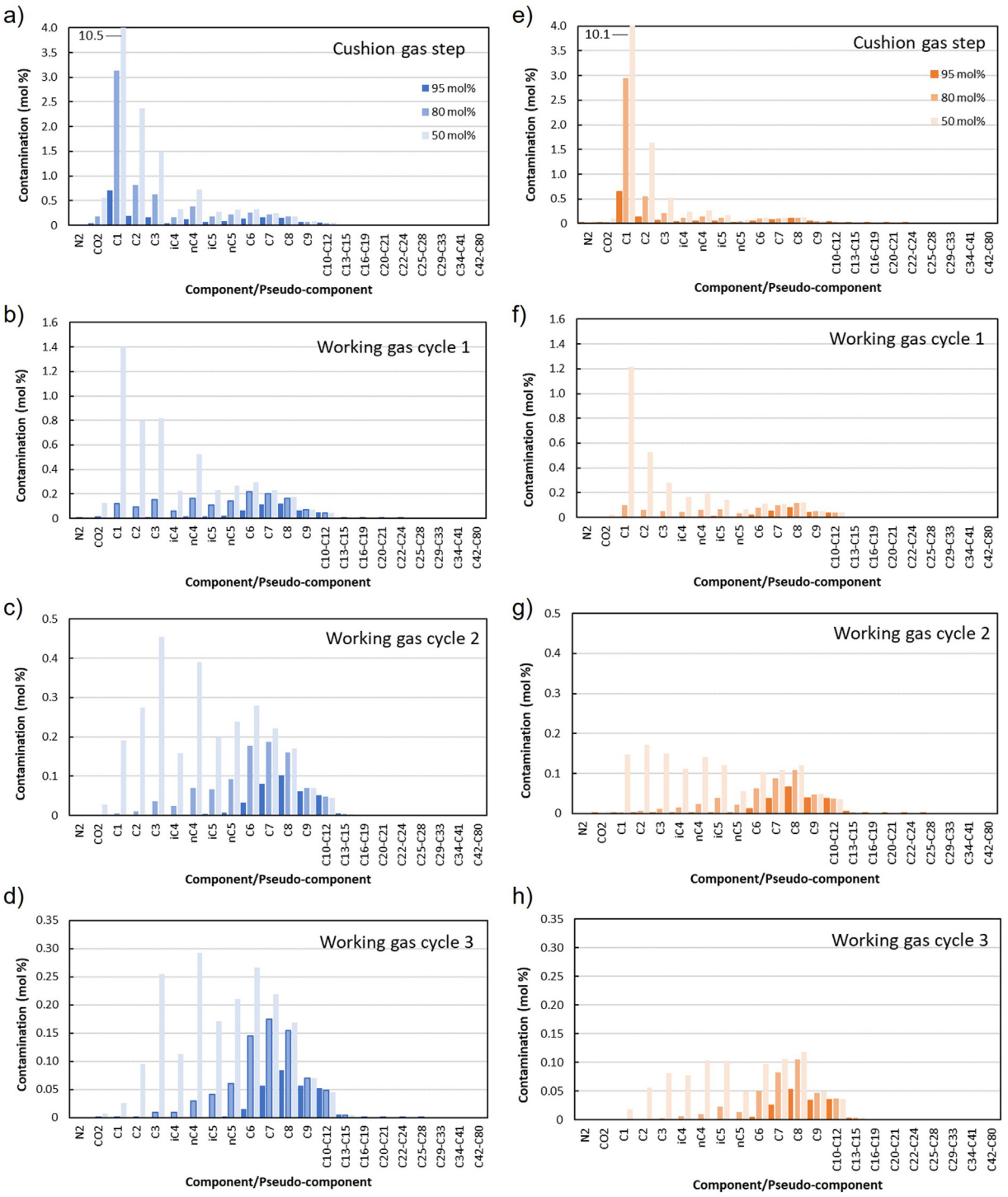

Fig. 4 – Component profile of hydrogen contamination in cushion gas step and first three working gas cycles in representative North Sea retrograde gas (a–d) and black oil (e–h) scenarios. The mol percentage numbers of the components and pseudo-components refer to the whole gas composition (but the dominant hydrogen content has been omitted to highlight the contamination part).

pacity estimates must be regarded as theoretical estimates as we neglect here water injection during O&G production, assume that the fully produced hydrocarbon volumes can be replaced by hydrogen, and do not include volumes needed for the usage of cushion gas.

The O&G reservoir depths vary from 1900 to 4200 m with temperatures between ca. 60 °C and 120 °C. The pressures scatter from 85 to 640 bar (pre- and post-production pressure data, see supplementary data). The caprock sequences are mainly 10–185 m layers of shale or variations of claystones.

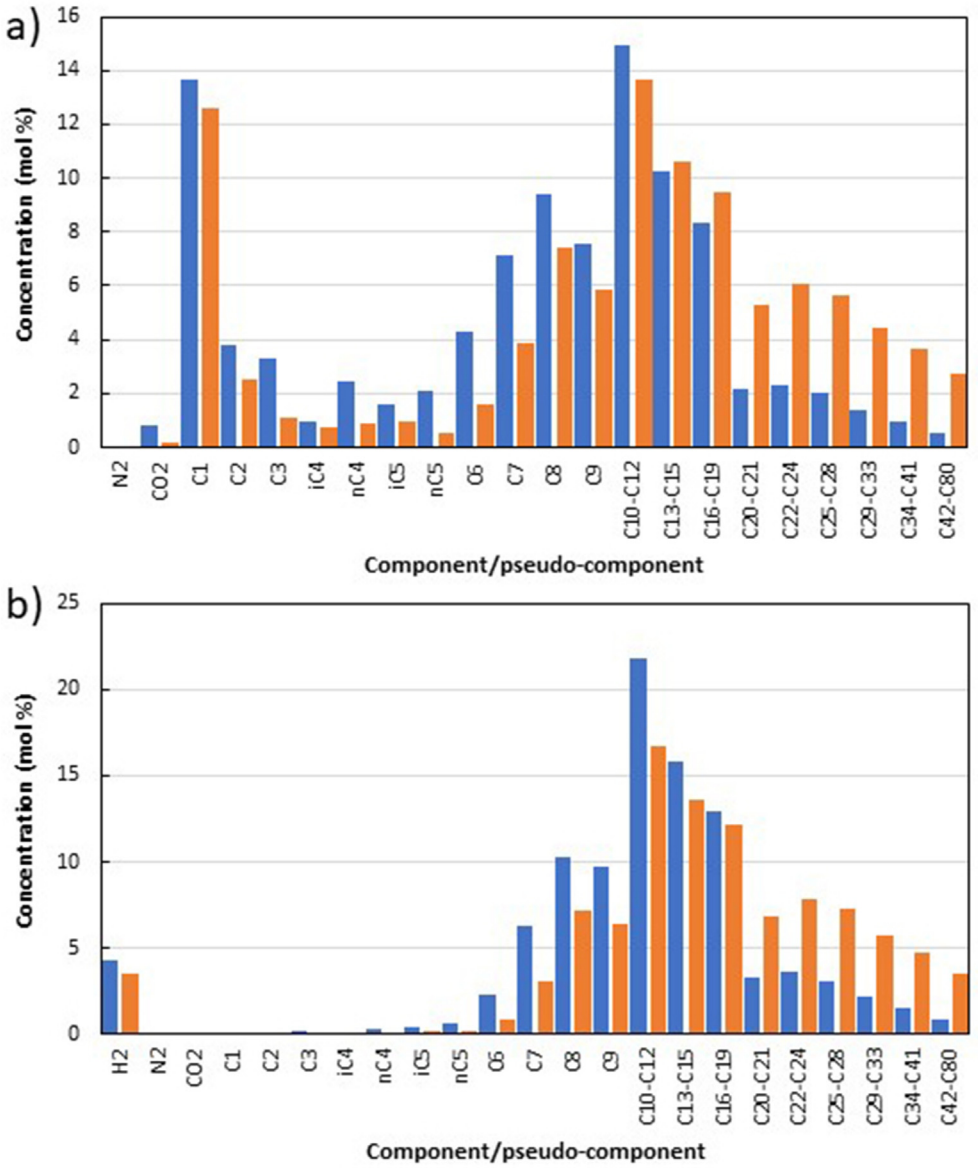

Fig. 5 – (a) The liquid phase composition in the representative North Sea retrograde gas (blue) and black oil (orange) scenarios. (b) The liquid phase composition of representative North Sea retrograde gas and black oil equilibrated for models R95H2 and BO95H2.

For the different fields, the storage capacities vary between ca. 0.01 Mt and 7.75 Mt, which equals heating capacities spanning between ca. 0.3 TWh and 305 TWh (Table 2). A field-specific description of the results and assumptions is provided in the supplementary data file.

Discussion

Hydrogen as an energy source and carrier has been identified as a pre-condition for the shift to a renewable energy network within Europe and to reach carbon net zero by 2050 [4], with the North Sea as an important energy storage and supply hub (Fig. 1). To substitute natural gas, a constant hydrogen supply must be guaranteed; hence cyclical, seasonal storage must be provided to cover peak demand and allow electrolysers to operate flexibly [4]. Furthermore, strategic hydrogen storage can secure energy supply in times of conflict. The best option to store GWh to TWh of hydrogen is UHS in salt caverns, saline aquifers, and depleted O&G fields. The advantages and disadvantages of UHS in salt caverns and saline aquifers are discussed in recent publications, and we refer to these for detailed information [8,9]. The re-usage of shut down O&G fields provides a promising solution to enable large-scale UHS storage within the next decade. Herein, we discuss some key features for hydrogen storage of the shut down O&G fields on the NCS and conclude by identifying the most suitable for UHS.

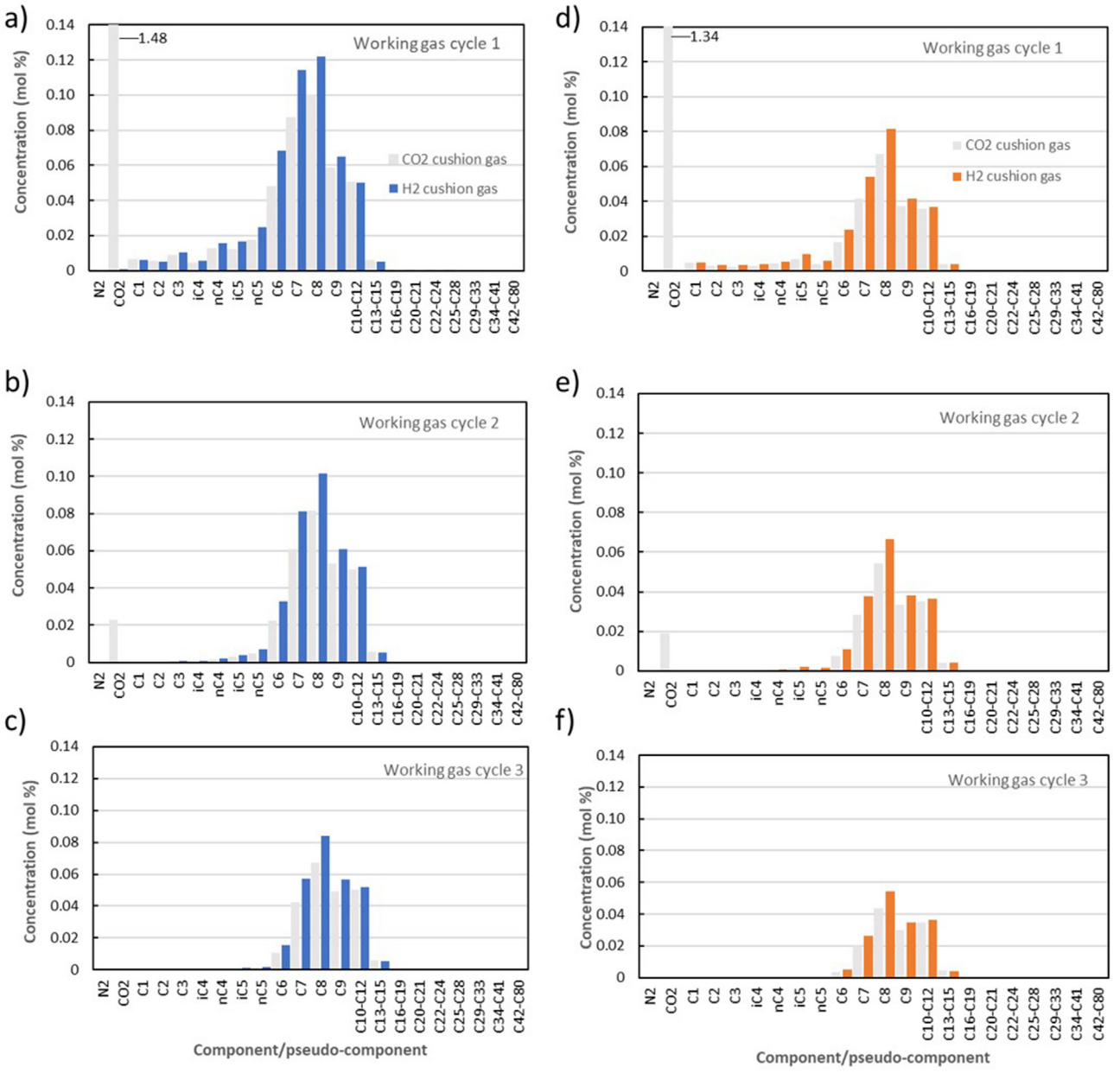

Fig. 6 – Contamination component profile for the first three working gas cycles using hydrogen (blue and orange) or CO_2 (grey) as a cushion gas for the 95 mol % hydrogen scenarios. Results for the retrograde gas field (a–c) and black oil field (d–f).

Geochemical considerations of hydrogen reactions and equilibrium phases

At first, we elaborate on the chemical reactions between hydrogen and hydrocarbon-bearing residual fluids. At the end of a production life-cycle of a hydrocarbon field, residual fluids remain in the depleted fields [22]. When hydrogen is injected into the pores of water-saturated reservoir rocks, it replaces the formation fluid (including residual hydrocarbons) and changes the *in-situ* chemical equilibrium. The displacement patterns are controlled by the fluid and rock properties (fluid viscosity and density, miscibility, wettability, pore features, etc.). Geochemical reactions can cause loss of hydrogen, contamination of the stored hydrogen (by e.g., H_2S), affect well activity by mineral dissolution/precipitation, and change migration pathways by changing mechanical properties of the reservoir and caprock [37].

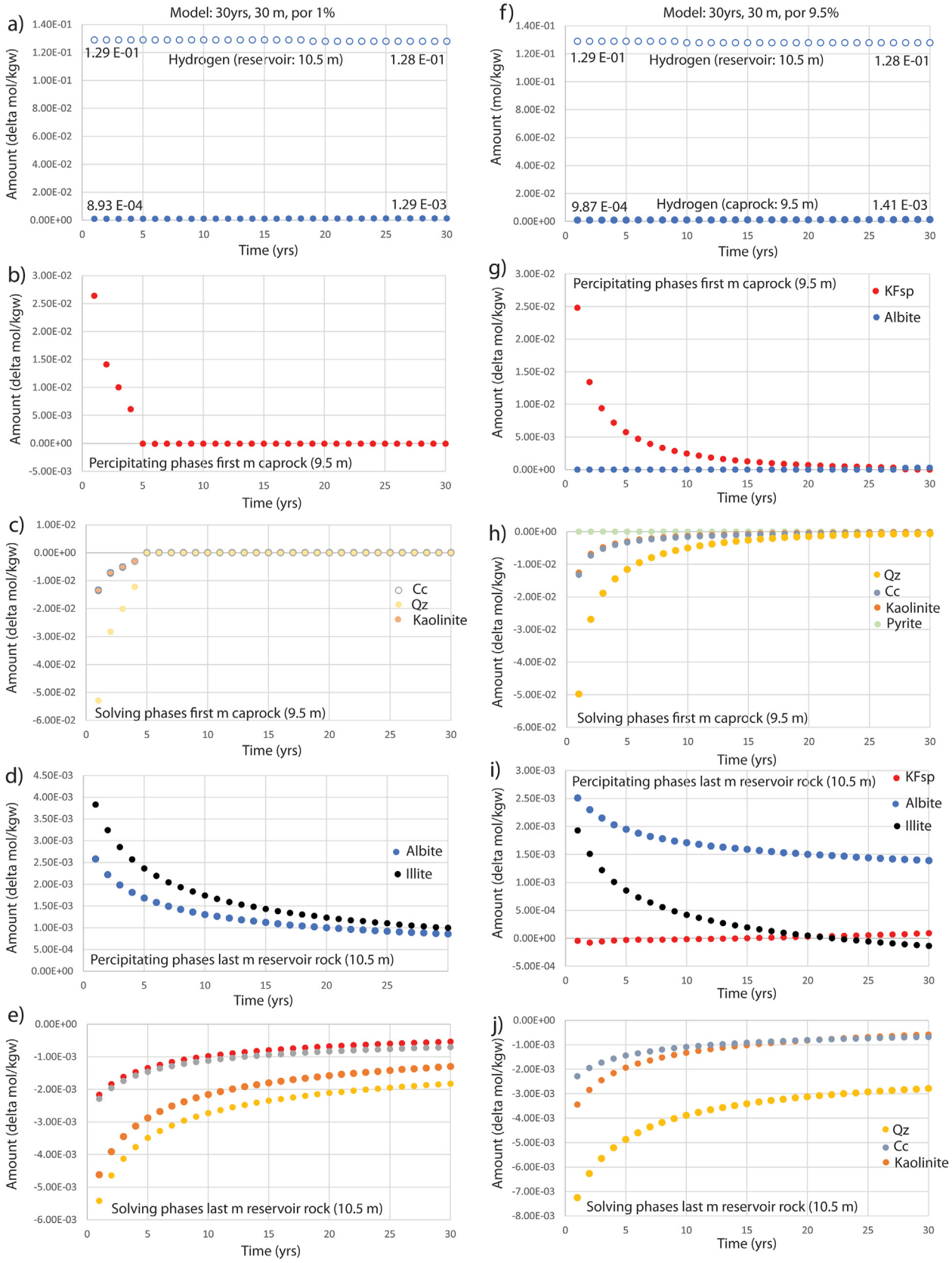

Fig. 7 – PHREEQC modelling results showing hydrogen concentration and selected mineral reactions over 30 yrs assuming a caprock porosity of 1% (a–e) and 9.5% (f–j). The precipitating and solving mineral phases are shown for the caprock/reservoir rock boundary at a model depth of 10.5 m (the last meter of the reservoir unit and the first meter of the caprock unit at 9.5 m).

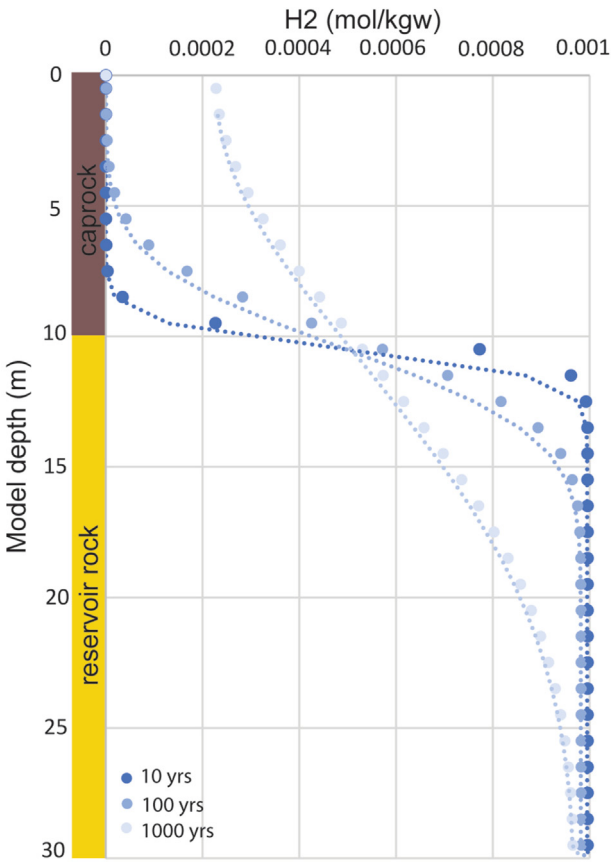

Fig. 8 – PHREEQC modelling results showing hydrogen diffusion after 10, 100 and 1000 years from the reservoir rock (10–30 m) into a caprock (0–10 m), assuming a porosity of 5% and a hydrogen tracer diffusion coefficient of 5.13 x 10^{-9} m^2/s (diffusion in pure water from [18]). The initial hydrogen concentration in the reservoir unit is fixed at 0.001 mol/kgw and 0 in the caprock.

Hydrogen equilibrium with residual hydrocarbons

Oil fields are typically regarded as not suitable for hydrogen storage because of possible working gas contamination and thus extra costs for top side hydrogen purification [8,40]. This hypothesis is partly examined by the presented thermodynamic equilibrium models suggesting moderate contamination levels. The models, however, are based on a few assumptions that might not represent a real-case storage scenario.

The PVTSIM modelled equilibration process assumes bulk mixing, whereas more realistic equilibration between hydrogen and hydrocarbon residues in the reservoir depends on pore network properties and fluid distribution. In the reservoir, the interaction between hydrogen and hydrocarbon residues may be more limited than indicated by the bulk mixing simulations. For that reason, the contamination levels derived from the mixing ratios should be considered upper bound estimates. On the other hand, the reservoir pressure is not constant during the injection of cushion gas and the following working gas cycles. The solubility of hydrogen and hydrocarbon liquid residues increases with increasing pressure. The simulations reported here assume for simplicity a constant low reservoir pressure of 50 bar. The simulations will therefore probably underestimate the effective contamination level of the hydrogen gas (which will vary during hydrogen cycling).

In the presented PVTSIM models, we assume hydrogen (or CO_2) injection as cushion gas before injecting hydrogen as a working gas. The cushion gas displaces the original reservoir fluid phase from the reservoir volume around the injector. A mixing zone between the original reservoir gas and cushion gas moves outwards from the injector as new cushion gas is injected. Upon migration, the cushion gas extracts different hydrocarbon components from the residual phases (Fig. 4a, e). Fig. 3 shows a significant difference between the contamination level in the cushion gas injection and the following working gas cycles. The cushion gas extracts and removes a large part of the more volatile components of the residual hydrocarbon liquid phase. Depending on the composition of the residual fluid, the extracted part can contain heavier hydrocarbon components from the residual liquid hydrocarbon phase in the pore space (Fig. 4a, e). In our models, maximum hydrogen losses to the residual liquid phase are approximately 4 mol % (Fig. 5). The results indicate that the working gas phase can be contaminated with light to medium weight hydrocarbon components (C1 to C12), with most models indicating less than 1 mol % of contamination from the different hydrocarbon components (Fig. 6). If CO_2 is used as a cushion gas, the produced working gas will additionally contain CO_2 contaminations in the first working gas cycles (Fig. 6). Models show that the total contamination level is remarkably similar for the retrograde gas and black oil fields (Fig. 3). Fractions of the injected hydrogen cushion gas is lost to the liquid hydrocarbon residues. Losses of hydrogen to the residual hydrocarbon increase with reservoir pressure and are higher for a retrograde gas residual fluid compared to a black oil residual fluid (Fig. 9). After the hydrocarbon residues are saturated, there is no significant loss of hydrogen in the subsequent working gas cycles. However, the mass of hydrogen loss depends on the amount of liquid hydrocarbon residues near the injector that can equilibrate with the injected hydrogen. In contrast to a gas field, a depleted oil field contains higher amounts of hydrocarbon residues. Thus, despite a similar mol percentage of hydrogen loss and contaminating hydrocarbon components in the presented PVTSIM results (Figs. 4–8), this would cause higher total volumes of hydrogen losses and contamination in the depleted black oil reservoirs compared to retrograde gas reservoirs.

Hydrogen reactions with reservoir rocks, caprocks and formation water

Besides residual hydrocarbons, the reservoir rock formation water and injected production water will be in contact with hydrogen. We focus on sandstone reservoirs because 19 out of 23 of the discussed reservoirs are in sandstones sealed by clay/shale. The main major minerals are silicates (quartz), clay minerals (kaolinite, illite) and carbonates (calcite). Various secondary minerals constitute specific reservoir units (e.g., pyrite). Injected hydrogen will react with the formation water and increase the pH [18,27,41]. In our simulations, pH increased in the caprock brine from ca. 7 to 8.7. The change in the geochemical equilibrium can cause mineral dissolution or

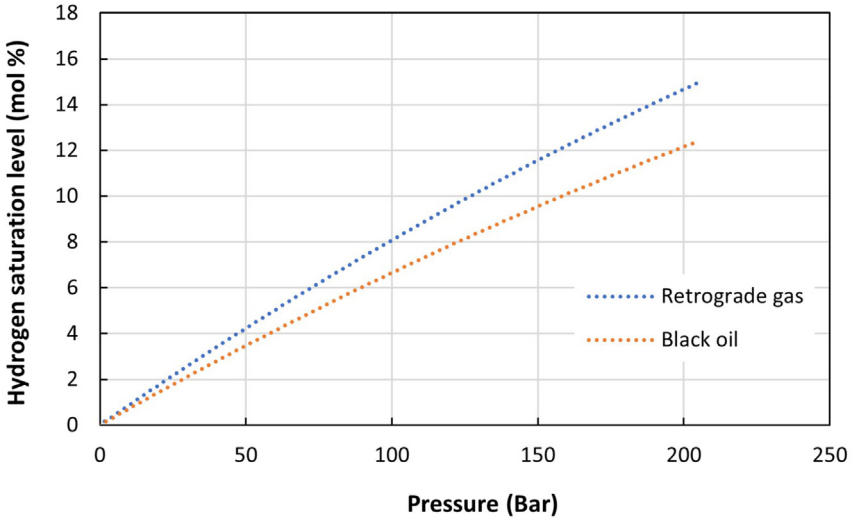

Fig. 9 – Saturation level of hydrogen in residual hydrocarbon liquid phase in cushion gas injection.

precipitation depending on pressure-temperature conditions, reservoir rock composition and formation water compositions [18]. We point out that geochemical model results for sandstones might not be reproduced in laboratory batch experiments as exemplified on calcite [42]. However, because sandstone is mostly composed of slow reacting minerals (e.g., quartz in our models 54 wt %). Such long termed models might not be reproducible by short-termed core-scale experiments using the standard kinetics of these slow reacting minerals [43].

One major uncertainty in hydrogen storage is the increase/decrease of porosities and permeabilities in the caprock and reservoir units by mineral reactions. Our models suggest several phases of minerals dissolution (mainly quartz, calcite, and kaolinite) and precipitation (mainly albite, illite and kali-feldspar). We did not quantify the total volumes of dissolved and precipitated mineral phases but amounts in mol/kgw suggest negligible amounts. Yeka et al. [44] studied the reactivity of hydrogen in sandstone at PT conditions of max 100 bar and 100–200 °C. In summary, the experimental results indicate extremely limited modifications of sandstone minerals after exposure to hydrogen for up to 6 months. However, after longer hydrogen exposure, muscovite and hematite (Fe_2O_3) are chemically modified due to reactions of Fe^{3+}. Long-term geochemical simulations point to the accelerated dissolution of hematite and magnetite (Fe_3O_4) and the necessity to map and quantify the concentration of Fe-bearing minerals in the reservoir and caprock units. Another major risk concerns impurities in the upstream product. The risks of hydrogen storage in depleted O&G fields include the conversion of hydrogen to CH_4 and H_2S due to microbial activity and gas–water–rock interactions in the reservoir and caprock. A study by Truche et al. [41] showed that 2 wt % of pyrite (FeS_2) can lead to H_2S in a reaction with hydrogen via reduction to pyrrhotite (FeS_{1+x}) in a calcite buffered system. In the absence of catalysts, most redox reactions caused by hydrogen remain insignificant at low temperatures. Our models assume 2.1 wt % of pyrite in the caprock unit, but reactions remained insignificant. However, in seven of the evaluated fields, pyrite is observed in the caprock or reservoir unit (supplementary data Table 3). A geochemical modelling study (based on PHREEQC) indicated that geochemical reactions associated with hydrogen dissolution in formation waters would be negligible for hydrogen loss reacting with silicate and clay minerals [45]. Additionally, recent laboratory batch reaction experiments with several types of reservoir sandstones revealed no risk of hydrogen loss or reservoir integrity degradation due to inorganic geochemical reactions [46].

Due to its small molecular size and very low density (0.08988 g/l at STP), hydrogen diffuses easily and therefore requires gas-tight storage conditions; for UHS this means reservoirs with excellent seal [11]. Caprocks in the southern North Sea are mainly shales and claystones from different formations. One of the best-described caprock unit is the mudrock of the Draupne Fm.: mineralogical composition [30] indicates that >50 wt % of the rock relates to the clay fraction (kaolinite, smectite and illite). The results of our geochemical simulations show that in a 0–100 yrs time scale, hydrogen may diffuse into the first 5 m of a Draupne type shale caprock unit. According to the model predictions, hydrogen will diffuse through a 10 m thick shale caprock unit in a 1000 yrs time-scale. In these models, permanent hydrogen saturation is assumed, which is unrealistic for storage projects with cyclic injection and production. However, the results of hydrogen diffusion models suggest using a minimum shale caprock thickness of 20 m. Hemme and Berk [18] modelled the hydrogeochemical mechanisms of storage at 160 atm and 80 °C, involving the reactions of bacterial metabolism, focusing on the hydrogen diffusion through a 180 m thick caprock for 30 yrs and 300 yrs. Their results indicate that hydrogen accumulated in the lower 4 m of the caprock after 30 yrs, and hydrogen reached the lower 10 m after 300 yrs, with a slight decrease in reservoir porosity due to mineral reactions. However, they calculated a loss of 25% of aqueous hydrogen by diffusion into the caprock after 30 yrs. Experiments from Wolff Boenisch et al. [47] suggest that hydrogen adsorption is temperature dependent but generally weak. They expect a hydrogen saturation in a clay caprock of 3–6 μl/

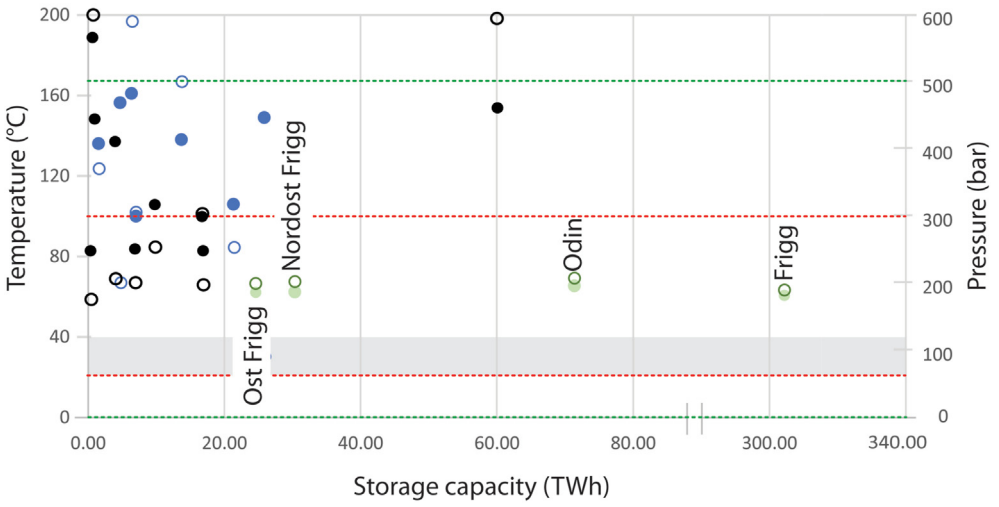

Fig. 10 – Black oil (black), gas (green) and gas prone (blue) fields storage capacities in relation to reservoir temperature (filled circles) and pressure (open circles). The red dashed line indicates the suggested temperature range from 20 to 100 °C [49–51], and the green dashed line the suggested pressure range from 1 to 500 bar [49] for hydrogen storage. Grey shaded area is the temperature range with the best microbial growth conditions [54].

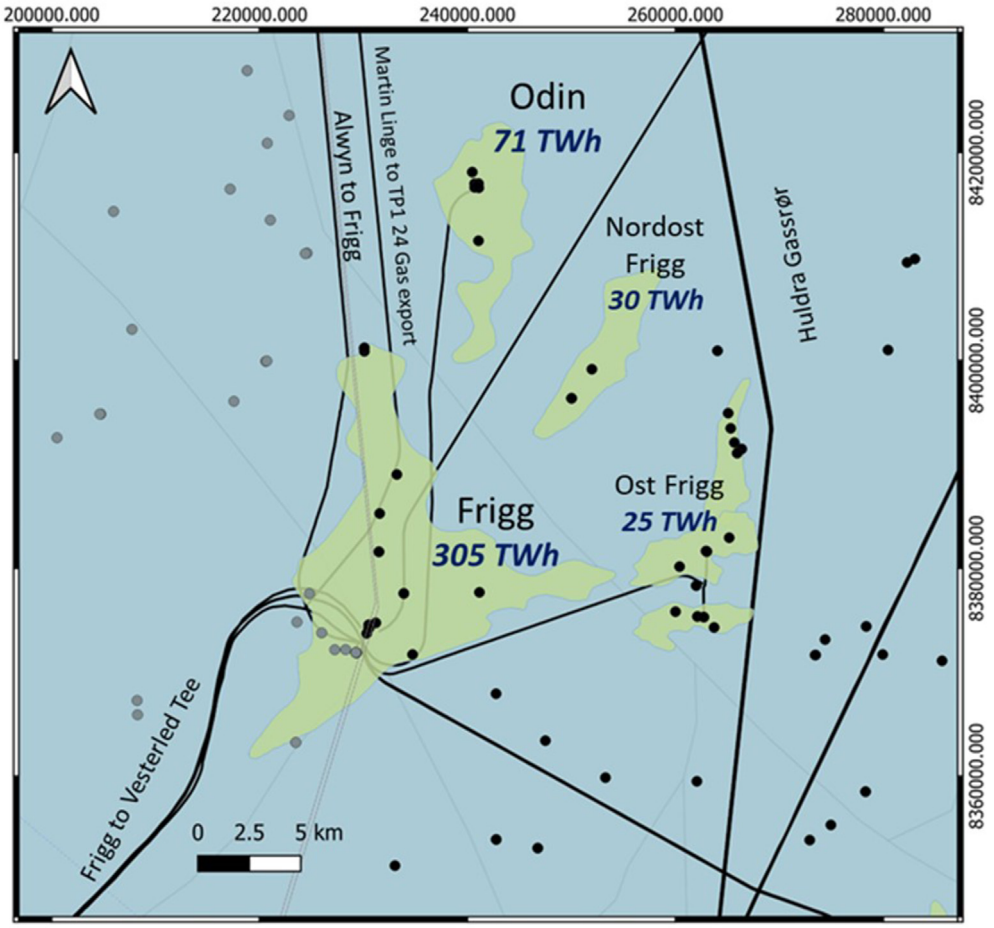

Fig. 11 – The area around the Frigg gas field with maximum UHS capacities given in TWh and infrastructure (partly legacy infrastructure) located around the fields. Black dots are well locations within the Norwegian economic zone, grey dots well bores within the British economic zone and black lines are pipelines.

m^2. Liu et al. [48] found the self-diffusion coefficient of 10^{-8} m^2/s (0.32 m/yr) for hydrogen in clay attain-situ conditions. Increasing temperature and slit aperture increase diffusion moderately. This diffusion coefficient is higher than assumed in our models.

The mineralogical reactions are complex and depend on model assumptions such as reactive mineral amounts, PT conditions, reservoir, caprock and brine compositions [18]. Furthermore, many mineral reactions occurring in equilibrium batch models will not occur in short-time intervals [27]. To obtain more realistic geochemical reaction models, samples from specific fields must be analysed and used as a model input parameter.

Pressure and temperature (PT) conditions for hydrogen storage and microbial side effects

The optimum PT for UHS have been defined as pressures between 1 and 500 bar [49] and temperatures of 20 °C to 100 °C related to the recommended depth range from 500 m to 2000 m in depleted O&G fields and saline aquifers [49–51]. This might be an oversimplification because geothermal gradients and pressure distribution vary significantly in sedimentary basins [52,53]. Other processes threatening successful hydrogen storage are methanogenesis, homoaceto genesis, and sulphate reduction of hydrogen in the subsurface [40,54,55]. Low-temperature reservoirs (<70 °C), with a low saline reservoir brine (0–0.6 M NaCl) and close to neutral pH values, provide the optimal conditions for microbial growth. The subsurface microorganisms can use hydrogen in their metabolism, causing hydrogen loss into hydrogen sulfide, methane and acid formation [55]. Biotic hydrogen consumption might be limited at temperatures >122 °C and higher brine salinities (>4.4 M NaCl). However, compared to other factors (e.g., the amount of needed cushion gas), the hydrogen loss with >0.001–3.2% is negligible [54]. Microorganisms are used for enhanced oil recovery [56] also in Norwegian hydrocarbon fields [57]. However, microbial activity or usage of bacteria for enhanced oil recovery are not reported in publicly available data and thus not included in our evaluation process. The possibility of countermeasures against microbial-related hydrogen losses, such as biocides or specific inhibitors against single metabolic groups, are under research [55]. A recent micro-CT imaging study of hydrogen displacement and trapping in a sandstone (at 2–7 MPa) indicates that higher pressure is less favourable for hydrogen storage because higher percentages of hydrogen are trapped in the pore space [58].

Taking these conditions into account, it seems that the Glitne, Jette, Jotun, Varg (black oil fields) and the Frigg, Odin, Nordost Frigg, and Yttergryta (retrograde gas and gas fields) are most suitable for hydrogen storage (Fig. 10).

Maximum underground hydrogen storage capacities

A maximum UHS capacity of ca. 642 TWh is estimated for all shut down fields. However, this sum contains fields which might not be optimal for hydrogen storage. The suitable black oil fields (Glitne, Jette, Jotun, Varg) have a combined maximum UHS capacity of 40.53 TWh. The new PVTSIM results indicate that hydrogen contamination due to residual oils in such fields would be similar to retrograde gas fields (Figs. 4–6). However, the simplistic model we employed glosses over an array of possible practical problems [37]. For example, black-oil reservoirs may pose other challenges, such as a higher risk of chemical interaction between hydrogen and hydrocarbon components [40]. The larger quantities of complex hydrocarbon components in black oil increase the risk of hydrogen getting lost in chemical reactions. If economically feasible, techniques can be used to purge hydrogen stored in depleted black-oil reservoirs.

Taking only suitable gas fields into account (Frigg, Nordost Frigg, Ost Frigg, and Odin) 432 TWh can be stored (Fig. 11; Table 2). The presented geochemical models suggest hydrogen diffusion into the first 5 m of the caprock after 100 yrs (Fig. 8). Thus, the caprock thickness of Ost Frigg with 10 m? might not be sufficient to guarantee economic and safe hydrogen storage. Excluding Ost Frigg, the remaining shut down gas fields could store hydrogen with an energy equivalent of 414 TWh. All these estimates do not include the amount of cushion gas required to maintain operational pressure and desired production rates [37]. In depleted gas fields, the amount of needed cushion gas is ca. 20–50% of the total available gas volume. For an economically feasible hydrogen storage project, cheaper gases such as CO_2 (Fig. 6), N_2, or natural gas can be used as cushion gas. Models using natural gas obtained 95% hydrogen recovery factors with minimal amounts of mixing in the reservoir [59]. Also, the equilibrium models presented here indicate that impurities are similar to hydrogen cushion gas (Fig. 6). However, to calculate the amount of working gas, the amount of cushion gas must be estimated correctly [37], and detailed dynamic reservoir models must be used to estimate the practicality of each field [60]. Using 20–50% cushion gas volume as a first estimate, the combined working gas volumes for the Frigg, Nordost Frigg, and Odin are in the range of 331 to 207 TWh. This is the range of Norway's 2020 energy consumption of 211 TWh [61]. Additionally, these fields have a below average well density between 0.46 and 0.6 (supplementary data Table 3), indicating that potential plugging and abandonment costs for legacy wells will be below average.

Conclusion

Twenty-three Norwegian shut down O&G fields have been evaluated for their hydrogen storage potential using publicly available data assisted by generic thermodynamic equilibrium and geochemical modelling. Generic thermodynamic equilibrium models and geochemical models explain the contamination potential and possible mineral reactions in a sandstone reservoir with residual hydrocarbons sealed by a shale caprock. The total hydrogen losses during different injection/production cycles must be evaluated by case-specific reservoir models.

The maximum UHS capacity in the Norwegian shut down O&G fields has an energy equivalent of 642 TWh. Considering more reasonable reservoir conditions suitable for feasible hydrogen storage, three wet gas fields are our recommended storage locations: Frigg field with a maximum UHS of ca.

306 TWh, Nordost Frigg field with 30 TWh and Odin field with 71 TWh. From these estimates, 50–80% can be used as working gas. This energy storage capacity would be sufficient to satisfy the energy needs of Norway for a year.

Declaration of competing interest

The authors declare that they have no known competing financial interests or personal relationships that could have appeared to influence the work reported in this paper.

Acknowledgement

This work was funded by the Research Council of Norway in the framework of the HySTORM - Clean offshore energy by hydrogen storage in petroleum reservoirs Researcher Project, grant number 315804.

Appendix A. Supplementary data

Supplementary data to this article can be found online at https://doi.org/10.1016/j.ijhydene.2023.03.138.

REFERENCES

[1] Fuss S, Canadell JG, Peters GP, Tavoni M, Andrew RM, Ciais P, et al. Betting on negative emissions. Nat Clim Change 2014;4:850–3. https://doi.org/10.1038/nclimate2392.
[2] Cruz MRM, Fitiwi DZ, Santos SF, Catalão JPS. A comprehensive survey of flexibility options for supporting the low-carbon energy future. Renew Sustain Energy Rev 2018;97:338–53. https://doi.org/10.1016/j.rser.2018.08.028.
[3] Raynaud D, Hingray B, François B, Creutin JD. Energy droughts from variable renewable energy sources in European climates. Renew Energy 2018;125:578–89. https://doi.org/10.1016/j.renene.2018.02.130.
[4] Communication From The Commission To The European Parliament, The Council. THE EUROPEAN ECONOMIC AND SOCIAL COMMITTEE AND THE COMMITTEE OF THE REGIONS A hydrogen strategy for a climate-neutral Europe. 2020.
[5] Feldmann F, Hagemann B, Ganzer L, Panfilov M. Numerical simulation of hydrodynamic and gas mixing processes in underground hydrogen storages. Environ Earth Sci 2016;75:1165. https://doi.org/10.1007/s12665-016-5948-z.
[6] Miocic JM, Alcalde J, Heinemann N, Marzan I, Hangx S. Toward energy-independence and net-zero: the inevitability of subsurface storage in Europe. ACS Energy Lett 2022:2486–9. https://doi.org/10.1021/acsenergylett.2c01303.
[7] Phillips R, Dunnill CW. Zero gap alkaline electrolysis cell design for renewable energy storage as hydrogen gas. RSC Adv 2016;6:100643–51. https://doi.org/10.1039/C6RA22242K.
[8] Scafidi J, Wilkinson M, Gilfillan SMV, Heinemann N, Haszeldine RS. A quantitative assessment of the hydrogen storage capacity of the UK continental shelf. Int J Hydrogen Energy 2021;46:8629–39. https://doi.org/10.1016/j.ijhydene.2020.12.106.
[9] Caglayan DG, Heinrichs HU, Robinius M, Stolten D. Robust design of a future 100% renewable european energy supply system with hydrogen infrastructure. Int J Hydrogen Energy 2021;46:29376–90. https://doi.org/10.1016/j.ijhydene.2020.12.197.
[10] Muhammed NS, Haq B, Al Shehri D, Al-Ahmed A, Rahman MM, Zaman E. A review on underground hydrogen storage: insight into geological sites, influencing factors and future outlook. Energy Rep 2022;8:461–99. https://doi.org/10.1016/j.egyr.2021.12.002.
[11] Heinemann N, Booth MG, Haszeldine RS, Wilkinson M, Scafidi J, Edlmann K. Hydrogen storage in porous geological formations – onshore play opportunities in the midland valley (Scotland, UK). Int J Hydrogen Energy 2018;43:20861–74. https://doi.org/10.1016/j.ijhydene.2018.09.149.
[12] Portarapillo M, Di Benedetto A. Risk assessment of the large-scale hydrogen storage in salt caverns. Energies 2021;14:2856. https://doi.org/10.3390/en14102856.
[13] Pawar RJ, Bromhal GS, Carey JW, Foxall W, Korre A, Ringrose PS, et al. Recent advances in risk assessment and risk management of geologic CO2 storage. Int J Greenh Gas Control 2015;40:292–311. https://doi.org/10.1016/j.ijggc.2015.06.014.
[14] Gasda SE, Bachu S, Celia MA. Spatial characterization of the location of potentially leaky wells penetrating a deep saline aquifer in a mature sedimentary basin. Environ Geol 2004;46:707–20. https://doi.org/10.1007/s00254-004-1073-5.
[15] Romdhane A, Emmel B, Zonetti S, Dupuy B, Gawel K, Edvardsen L, et al. Screening, monitoring, and remediation of legacy wells to improve reservoir integrity for large-scale CO2 storage—an example from the smeaheia structure in the northern North Sea. Front Energy Res 2022:10.
[16] Alcalde J, Flude S, Wilkinson M, Johnson G, Edlmann K, Bond CE, et al. Estimating geological CO2 storage security to deliver on climate mitigation. Nat Commun 2018;9:2201. https://doi.org/10.1038/s41467-018-04423-1.
[17] Heinemann N, Alcalde J, Miocic JM, Hangx SJT, Kallmeyer J, Ostertag-Henning C, et al. Enabling large-scale hydrogen storage in porous media – the scientific challenges. Energy Environ Sci 2021;14:853–64. https://doi.org/10.1039/D0EE03536J.
[18] Hemme C, van Berk W. Hydrogeochemical modeling to identify potential risks of underground hydrogen storage in depleted gas fields. Appl Sci 2018;8:2282. https://doi.org/10.3390/app8112282.
[19] Deronzier J-F, Giouse H. Vaux-en-Bugey (Ain, France): the first gas field produced in France, providing learning lessons for natural hydrogen in the sub-surface? Bull Soc Geol Fr 2020;191:7. https://doi.org/10.1051/bsgf/2020005.
[20] Shut down - Factpages - Npd n.d. https://factpages.npd.no/en/field/PageView/ShutDown (accessed August 10, 2022).
[21] Holloway S, Rochelle C, Bateman K, Pearce J, Baily H, Metcalfe R. The underground disposal of carbon dioxide : final report. Nottingham, UK: British Geological Survey; 1996.
[22] Blunt M, Fayers FJ, Orr FM. Carbon dioxide in enhanced oil recovery. Energy Convers Manag 1993;34:1197–204. https://doi.org/10.1016/0196-8904(93)90069-M.
[23] Mulyadi H. Determination of residual gas saturation and gas-water relative permeability in water-driven gas reservoirs. Thesis. Curtin University; 2002.
[24] Besancon BM, Hasanov V, Imbault-Lastapis R, Benesch R, Barrio M, Mølnvik MJ. Hydrogen quality from decarbonized fossil fuels to fuel cells. Int J Hydrogen Energy 2009;34:2350–60. https://doi.org/10.1016/j.ijhydene.2008.12.071.

[25] Cheng X, Shi Z, Glass N, Zhang L, Zhang J, Song D, et al. A review of PEM hydrogen fuel cell contamination: impacts, mechanisms, and mitigation. J Power Sources 2007;165:739–56. https://doi.org/10.1016/j.jpowsour.2006.12.012.
[26] Du Z, Liu C, Zhai J, Guo X, Xiong Y, Su W, et al. A review of hydrogen purification technologies for fuel cell vehicles. Catalysts 2021;11:393. https://doi.org/10.3390/catal11030393.
[27] Hassannayebi N, Azizmohammadi S, De Lucia M, Ott H. Underground hydrogen storage: application of geochemical modelling in a case study in the Molasse Basin, Upper Austria. Environ Earth Sci 2019;78. https://doi.org/10.1007/s12665-019-8184-5.
[28] Pedersen KS, Christensen PL. Phase Behavior of Petroleum Reservoir Fluids. CRC Press, Taylor & Francis Group; 2007. https://www.calsep.com/.
[29] Description of input and examples for PHREEQC version 3: a computer program for speciation, batch-reaction, one-dimensional transport, and inverse geochemical calculations n.d. https://pubs.er.usgs.gov/publication/tm6A43 (accessed August 9, 2022).
[30] Edvardsen L, Bhuiyan MH, Cerasi PR, Bjørge R. Fast evaluation of caprock strength sensitivity to different CO2 solutions using small sample techniques. Rock Mech Rock Eng 2021;54:6123–33. https://doi.org/10.1007/s00603-021-02641-6.
[31] Mørk MBE, Johnsen SO. Jurassic sandstone provenance and basement erosion in the Møre margin – Froan Basin area n.d.:14.
[32] Hemme C, van Berk W. Change in cap rock porosity triggered by pressure and temperature dependent CO2–water–rock interactions in CO2 storage systems. Petroleum 2017;3:96–108. https://doi.org/10.1016/j.petlm.2016.11.010.
[33] McCaine Jr WD. The properties of petroleum fluids, 2nd ed., PennWell, Tulsa, Oklahoma. Ch.5 (The Five Reservoir Fluids). n.d.
[34] All - Factpages - Npd n.d. https://factpages.npd.no/en/field/PageView/All (accessed August 10, 2022).
[35] Bergmo PES, Emmel BU, Anthonsen KL, Aagaard P, Mortensen GM, Sundal A. Quality ranking of the best CO2 storage aquifers in the nordic countries. Energy Proc 2017;114:4374–81. https://doi.org/10.1016/j.egypro.2017.03.1589.
[36] Thermophysical properties of fluid systems n.d. https://webbook.nist.gov/chemistry/fluid/(accessed August 10, 2022).
[37] Heinemann N, Scafidi J, Pickup G, Thaysen E, Hassanpouryouzband A, Wilkinson M, et al. Hydrogen storage in saline aquifers: the role of cushion gas for injection and production. Int J Hydrogen Energy 2021;46. https://doi.org/10.1016/j.ijhydene.2021.09.174.
[38] Torres R, Hemptinne J-C, Machin I. Improving the modeling of hydrogen solubility in heavy oil cuts using an augmented grayson streed (AGS) approach. Oil Gas Sci Technol 2013;68:217–33. https://doi.org/10.2516/ogst/2012061.
[39] Trinh T-K-H, de Hemptinne J-C, Lugo R, Ferrando N, Passarello J-P. Hydrogen solubility in hydrocarbon and oxygenated organic compounds. J Chem Eng Data 2016;61:19–34. https://doi.org/10.1021/acs.jced.5b00119.
[40] Zivar D, Kumar S, Foroozesh J. Underground hydrogen storage: a comprehensive review. Int J Hydrogen Energy 2021;46:23436–62. https://doi.org/10.1016/j.ijhydene.2020.08.138.
[41] Truche L, Jodin-Caumon M-C, Lerouge C, Berger G, Mosser-Ruck R, Giffaut E, et al. Sulphide mineral reactions in clay-rich rock induced by high hydrogen pressure. Application to disturbed or natural settings up to 250°C and 30bar. Chem Geol 2013;351:217–28. https://doi.org/10.1016/j.chemgeo.2013.05.025.
[42] Gelencsér O, Árvai Cs, Mika LT, Breitner D, LeClair D, Cs Szabó, et al. Effect of hydrogen on calcite reactivity in sandstone reservoirs: experimental results compared to geochemical modeling predictions. J Energy Storage 2023;61:106737. https://doi.org/10.1016/j.est.2023.106737.
[43] Khaledialidusti R, Kleppe J. Significance of the kinetics of minerals in reactive-transport problems. OnePetro; 2017. https://doi.org/10.2118/185844-MS.
[44] Yekta AE, Pichavant M, Audigane P. Evaluation of geochemical reactivity of hydrogen in sandstone: application to geological storage. Appl Geochem 2018;95:182–94. https://doi.org/10.1016/j.apgeochem.2018.05.021.
[45] Bo Z, Zeng L, Chen Y, Xie Q. Geochemical reactions-induced hydrogen loss during underground hydrogen storage in sandstone reservoirs. Int J Hydrogen Energy 2021;46:19998–20009. https://doi.org/10.1016/j.ijhydene.2021.03.116.
[46] Hassanpouryouzband A, Adie K, Cowen T, Thaysen EM, Heinemann N, Butler IB, et al. Geological hydrogen storage: geochemical reactivity of hydrogen with sandstone reservoirs. ACS Energy Lett 2022;7:2203–10. https://doi.org/10.1021/acsenergylett.2c01024.
[47] Wolff-Boenisch D, Abid HR, Tucek JE, Keshavarz A, Iglauer S. Importance of clay-H2 interactions for large-scale underground hydrogen storage. Int J Hydrogen Energy 2023. https://doi.org/10.1016/j.ijhydene.2022.12.324.
[48] Liu J, Wang S, Javadpour F, Feng Q, Cha L. Hydrogen diffusion in clay slit: implications for the geological storage. Energy Fuels 2022;36:7651–60. https://doi.org/10.1021/acs.energyfuels.2c01189.
[49] Shi Z, Jessen K, Tsotsis TT. Impacts of the subsurface storage of natural gas and hydrogen mixtures. Int J Hydrogen Energy 2020;45:8757–73. https://doi.org/10.1016/j.ijhydene.2020.01.044.
[50] Matos CR, Carneiro JF, Silva PP. Overview of large-scale underground energy storage technologies for integration of renewable energies and criteria for reservoir identification. J Energy Storage 2019;21:241–58. https://doi.org/10.1016/j.est.2018.11.023.
[51] Hassanpouryouzband A, Joonaki E, Edlmann K, Heinemann N, Yang J. Thermodynamic and transport properties of hydrogen containing streams. Sci Data 2020;7:222. https://doi.org/10.1038/s41597-020-0568-6.
[52] Pascal C. Heat flow of Norway and its continental shelf. Mar Petrol Geol 2015;66:956–69. https://doi.org/10.1016/j.marpetgeo.2015.08.006.
[53] Lothe A, Bergmo P, Emmel B, Eliasson P. Effects of uncertainties in fault interpretations on pressure depletion and CO2 storage injection at horda platform, offshore Norway. SSRN Electron J 2019. https://doi.org/10.2139/ssrn.3366363.
[54] Thaysen E, McMahon S, Strobel GJ, Butler I, Heinemann N, Ngwenya B, et al. Estimating microbial growth and hydrogen consumption in hydrogen storage in porous media. Renew Sustain Energy Rev 2021;151:111481. https://doi.org/10.1016/j.rser.2021.111481.
[55] Dopffel N, Jansen S, Gerritse J. Microbial side effects of underground hydrogen storage – knowledge gaps, risks and opportunities for successful implementation. Int J Hydrogen Energy 2021;46:8594–606. https://doi.org/10.1016/j.ijhydene.2020.12.058.
[56] Nikolova C, Gutierrez T. Use of microorganisms in the recovery of oil from recalcitrant oil reservoirs: current state of knowledge,

technological advances and future perspectives. Front Microbiol 2020;10.
[57] Awan AR, Teigland R, Kleppe J. EOR survey in the North Sea. OnePetro; 2006. https://doi.org/10.2118/99546-MS.
[58] Thaysen E, Butler I, Hassanpouryouzband A, Freitas D, Alvarez-Borges F, Krevor S, et al. Pore-scale imaging of hydrogen displacement and trapping in porous media. 2022. https://doi.org/10.31223/X54346.
[59] Scafidi J, Schirrer L, Vervoort I, Heinemann N. Compositional simulation of hydrogen storage in a depleted gas field. Copernicus Meetings; 2021. https://doi.org/10.5194/egusphere-egu21-7738.
[60] Lysyy M, Fernø M, Ersland G. Seasonal hydrogen storage in a depleted oil and gas field. Int J Hydrogen Energy 2021;46:25160–74. https://doi.org/10.1016/j.ijhydene.2021.05.030.
[61] Energy use by sector. Energifakta Norge n.d. https://energifaktanorge.no/en/norsk-energibruk/energibruken-i-ulike-sektorer/(accessed August 10, 2022).